Biochemical Pharmacology 96 (2015) 225–236

Contents lists available at ScienceDirect

Biochemical Pharmacology

journal homepage: www.elsevier.com/locate/biochempharm

Activation of AMPK by chitosan oligosaccharide in intestinal epithelial cells: Mechanism of action and potential applications in intestinal disorders

Chatchai Muanprasat [a,*], Preedajit Wongkrasant [a], Saravut Satitsri [a], Aekkacha Moonwiriyakit [a], Pawin Pongkorpsakol [a], Tharinee Mattaveewong [a], Rath Pichyangkura [b], Varanuj Chatsudthipong [a]

[a] Department of Physiology, Faculty of Science, Mahidol University, Rajathevi, Bangkok 10400, Thailand
[b] Department of Biochemistry, Faculty of Science, Chulalongkorn University, Phayathai, Bangkok 10330, Thailand

ARTICLE INFO

Article history:
Received 30 April 2015
Accepted 28 May 2015
Available online 3 June 2015

Keywords:
Chitosan oligosaccharide
Intestinal epithelial cells
AMP-activated protein kinase
Diarrhea
Colorectal cancer

ABSTRACT

Chitosan oligosaccharide (COS), a biomaterial derived from chitin, is absorbed by intestinal epithelia without degradation and has diverse biological activities including intestinal epithelial function. However, the mode of action is still unclear. This study aimed to investigate the effect of COS on AMP-activated protein kinase (AMPK) in intestinal epithelial cells (IEC) and its potential applications in the intestinal diseases benefited from AMPK activation. COS with molecular weights (MW) from 5,000 Da to 14,000 Da induced AMPK activation in T84 cells. That with MW of 5,000-Da was the most potent polymer and was used in the subsequent experiments. COS also activated AMPK in other IEC including HT-29 and Caco-2 cells. Mechanism of COS-induced AMPK activation in T84 cells involves calcium-sensing receptor (CaSR)-phospholipase C (PLC)-IP_3 receptor channel-mediated calcium release from endoplasmic reticulum (ER). In addition, COS promoted tight junction assembly in T84 cells in an AMPK-dependent manner. COS also inhibited NF-κB transcriptional activity and NF-κB-mediated inflammatory response and barrier disruption via AMPK-independent mechanisms. Interestingly, luminal exposure to COS suppressed cholera toxin-induced intestinal fluid secretion by ~30% concurrent with AMPK activation in a mouse closed loop model. Importantly, oral administration of COS prevented the development of aberrant crypt foci in a mouse model of colitis-associated colorectal cancer (CRC) via a mechanism involving AMPK activation-induced β-catenin suppression and caspase-3 activation. Collectively, this study reveals a novel action of COS in activating AMPK via CaSR-PLC-IP_3 receptor channel-mediated calcium release from ER. COS may be beneficial in the treatment of secretory diarrheas and CRC chemoprevention.

1. Introduction

AMP-activated protein kinase (AMPK), a heterotrimeric protein composed of α, β and γ subunits, is an energy sensor that controls energy homeostasis at both cellular and whole-body levels [1]. In response to increased ADP/ATP ratio or increased intracellular calcium concentration ($[Ca^{2+}]_i$), AMPK activity is enhanced through phosphorylation at threonine-172 (Thr-172) of AMPK-α subunit by liver kinase B1 (LKB1) or calcium/calmodulin-dependent protein kinase kinase β (CaMKKβ), respectively [1]. Upon its activation, AMPK phosphorylates target proteins and modulates their functional activities, leading to stimulation of energy-production processes and inhibition of energy-utilizing processes [1].

Apart from its role in controlling energy balance, AMPK regulates epithelial functions including tight junction assembly and ion transport [2–4]. For instance, AMPK promotes an assembly of tight junction proteins to apical junctional complexes in epithelial cells [5,6]. In addition, AMPK phosphorylates CFTR Cl^- channel, leading to suppression of CFTR channel activity [7]. Located in the apical membrane of intestinal epithelial cells

* Corresponding author. Tel.: +66 2 201 5615; fax: +66 2 354 7154.
E-mail address: chatchai.mua@mahidol.ac.th (C. Muanprasat).

http://dx.doi.org/10.1016/j.bcp.2015.05.016
0006-2952/

(IEC), CFTR mediates cAMP-induced Cl^- secretion. Hence, overstimulation of the CFTR-mediated Cl^- secretion by enterotoxins (e.g. cholera toxin or CT) plays important roles in providing a driving force for intestinal fluid secretion in secretory diarrheas [8]. AMPK activators including AICAR and metformin abrogated CT-induced fluid secretion in excised mouse intestinal loops [9]. Interestingly, AMPK activators retarded growth of colorectal cancer (CRC) cell lines and prevented colitis-associated carcinogenesis in mice by inducing caspase-3 cleavage-mediated apoptosis of cancer cells [10–12]. Of particular interest, AMPK activation in human intestinal tissues is associated with superior prognosis in CRC patients [13]. Therefore, AMPK has been proposed as a drug target for CRC chemoprevention [14].

Chitosan oligosaccharide (COS) is a degradation product of chitosan, a polymer of β-(1-4)-linked D-glucosamine, derived from deacetylation of chitin found in exoskeletons of shrimps, crabs and insects. Due to its water solubility, biocompatibility, intestinal absorbability, and bioactivity, COS has received considerable interest for potential applications as dietary supplements or nutraceuticals [15]. To date, COS possesses a variety of biological activities such as anti-oxidative, anti-inflammatory and anti-bacterial activities [15]. After ingestion, COS is not digested by either gastrointestinal enzymes or gut floras, but is readily absorbed through intestinal epithelium [16,17]. Therefore, it is crucial to investigate the effects of COS on IEC, which is directly exposed to ingested COS and plays pivotal roles in health and diseases. Indeed, COS has recently been shown by our group to alleviate inflammation and its associated damages in mouse models of inflammatory bowel disease through suppression of nuclear factor kappa B (NF-κB)-mediated inflammatory responses in IEC [18]. However, the effect of COS on AMPK, which is an important regulator of intestinal epithelial functions, has not yet been reported. Therefore, this study aimed to investigate the effects of COS on AMPK activity and the underlying mechanisms in IEC. Furthermore, COS was evaluated for its effect on barrier function and potential application in the treatment of secretory diarrheas and in the chemoprevention of CRC.

2. Materials and methods

2.1. Materials

T84, HT-29 and Caco-2 cells were obtained from American Type Culture Collection (Manassas, VA, USA). Cholera toxin (CT) was from List Biological Laboratories, Inc. (Campbell, CA, USA). Fetal bovine serum (FBS) and culture media were from Thermo Fisher Scientific Inc. (Waltham, MA, USA). Other chemicals were from Sigma–Aldrich Co. (Saint Louis, MO, USA).

2.2. Preparation of chitosan oligosaccharides

Chitosan oligosaccharides (COS) with molecular weight (MW) of 5000 Da, 8000 Da, and 14,000 Da, and chitosan with MW of ~100,000 Da (all at the degrees of deacetylation >90%) were prepared according to the protocol used in the previous study [18]. Molecular weight of COS was defined by gel permeation chromatography. Degree of deacetylation of COS was defined by UV spectroscopic method. COS was dissolved in 1% acetic acid.

2.3. Cell culture

T84 cells were cultured in a 1:1 mixture of Dulbecco's modified Eagle's medium (DMEM) and Ham's F-12 medium included with 5% FBS, 100 U/mL penicillin and 100 μg/mL streptomycin (Life Technologies, Carlsbad, CA, USA). Caco-2 and HT-29 cells were cultured in DMEM supplemented with 10% FBS, 1% non-essential amino acids, 100 U/mL penicillin and 100 μg/mL streptomycin. Cells were maintained in a humidified 95% O_2/5% CO_2 atmosphere at 37 °C.

2.4. Western blot analysis

Cells were seeded on 6-well plates at a density of 1×10^6 cells/well (Corning Life Sciences, Tewksbury, MA, USA). After treatments, cell lysates or mouse tissue lysates were harvested using lysis buffer. Protein concentrations in cell lysates were measured by Lowry method. Thirty-microgram proteins were separated using sodium dodecyl sulfate polyacrylamide gel electrophoresis (SDS-PAGE) before transferring to nitrocellulose membrane. The membrane was blocked for 1 h with 5% non-fat dried milk (Bio-Rad, Hercules, CA, USA), and incubated overnight with rabbit antibodies to phospho-AMPK (Thr-172), AMPKα, phospho-acetyl Co-A carboxylase (Ser-79) (p-ACC), acetyl Co-A carboxylase (ACC), inducible nitric oxide synthase (iNOS), cyclooxygenase 2 (COX-2), β-catenin, cleaved caspase-3, or β-actin (Cell Signaling Technology, Boston, MA, USA). The membrane was then washed for 4 times with Tris-Buffered Saline Tween-20 (TBST) and incubated for 1 hour at room temperature with horseradish peroxidase-conjugated goat antibody to rabbit immunoglobulin G (Cell Signaling Technology, Boston, MA, USA). The signals were detected using Luminata Crescendo Western HRP Substrate (Merck Millipore, Billerica, MA, USA). Densitometry analysis was performed using Image J software (version 1.46r, National Institute of Health, Bethesda, MD, USA).

2.5. Determination of ADP/ATP ratio

ADP/ATP ratio was determined using the ADP/ATP Ratio Assay Kit (bioluminescent, ab65313, Abcam, Cambridge, MA, USA). Briefly, T84 cells (5×10^3 cells/well) were cultured for 24 h in 96-well plates before 24-h treatment with COS (100 μg/mL), metformin (5 mM) or vehicle. Cell lysates were determined for ADP/ATP ratio according to the manufacturer's instructions. Luminescence was detected using a Wallac Victor^2 microplate reader (PerkinElmer, Waltham, MA, USA).

2.6. Intracellular calcium measurement

T84 cells were harvested and incubated for 1 h at 37 °C with 1 mM indo-1 (Life Technologies, Carlsbad, CA, USA). Cells were then washed with fresh buffer containing 0.441 mM KH_2PO_4, 5.33 mM KCl, 4.17 mM $NaHCO_3$, 5.56 mM D-glucose, 137.93 mM NaCl, 0.338 mM Na_2HPO_4, 1 mM $CaCl_2$ and 1% (w/v) BSA, or the buffer without $CaCl_2$ for 3 times. The mean fluorescence intensity ratio between Ca^{2+}-bound indo-1 (excitation wavelength of 338 nm, emission wavelength of 405 nm) and Ca^{2+}-free indo-1 (excitation wavelength of 338 nm, emission wavelength of 490 nm) was detected by an FP-6200 spectrofluorometer (JASCO, Essex, UK).

2.7. Assay of NF-κB transcriptional activity

T84 cells (2×10^5 cells/well) were seeded and grown overnight on a 24-well plate before 24-h incubation in Opti-MEM (Life Technologies, Carlsbad, CA, USA) containing NF-κB GFP reporter (Qiagen Inc., Valencia, CA, USA) and Lipofectin Transfection Reagent (Life Technologies, Carlsbad, CA, USA) (at the ratio of 50:1:3.33). Cells were then incubated for 6 h in DMEM/F-12 media containing vehicle, TNFα (10 ηg/mL), TNFα (10 ηg/mL) plus COS (100 μg/mL) with or without compound C (80 μM), or compound C (80 μM) alone. Cells were trypsinized and determined for GFP

fluorescence by flow cytometry (excitation wavelength of 488 nm, emission wavelength of 515 nm) (FACS Canto, BD Biosciences, San Jose, CA, USA). Mean fluorescence intensity was used as an indicator of NF-κB transcriptional activity.

2.8. Measurement of tight junction assembly

The integrity of epithelial tight junction was determined by two methods, Ca^{2+} switch assay and FITC-dextran flux. For Ca^{2+} switch assay, T84 cells were seeded on a Transwell permeable support (5×10^5 cells/support) (Corning Life Sciences, Tewksbury, MA, USA) and cultured for 3 days. Then, culture media were removed and replaced with the Minimum Essential Medium Eagle, Spinner Modification (S-MEM), Ca^{2+}-free culture media, to disrupt tight junctions. Sixteen hours later, S-MEM medium was replaced with regular T84 cell medium (DMEM/Ham's F-12) containing Ca^{2+} ("Ca^{2+} switch") supplemented with vehicle, COS (100 μg/mL), COS (100 μg/mL) plus compound C (80 μM), or compound C (80 μM) alone. Transepithelial electrical resistance (TEER) was measured before and after (1, 6, 12 and 24 h) Ca^{2+} switch using EVOM^2 volt-ohm meter (World Precision Instruments, Inc., Sarasota, FL, USA). In some experiments, TEER was measured without Ca^{2+} switch.

For FITC-dextran flux assay, T84 cells were seeded on a Transwell permeable support (5×10^5 cells/support) and cultured for 7 days. Then, T84 cell monolayers were treated for 24 h with vehicle, compound C (80 μM), TNFα (10 ηg/mL), TNFα (10 ηg/mL) plus COS (100 μg/mL) or TNFα (10 ηg/mL) plus COS (100 μg/mL) and compound C (80 μM). FITC-dextran (MW ~4,400 Da) was added into the apical media (1 mg/mL) and, an hour later, basolateral media was sampled for the determination of FITC-dextran concentration using a Wallac Victor^2 microplate reader (PerkinElmer, Waltham, MA, USA).

2.9. Mouse model of cholera toxin-induced intestinal fluid secretion

After 24 h of fasting, mice were anesthetized by intraperitoneal injection of thiopenthal sodium (50 mg/kg), followed by abdominal incision and isolation of 3 closed ileal loops (2–3 cm long) by sutures. Ileal loops were instilled with 100 μL of phosphate-buffered saline (PBS) or PBS containing cholera toxin (1 μg/loop) with or without COS (100 μg/mL). Four hours later, mice were re-anesthetized and ileal loops were removed for measurements of weight/length ratio. The experimental protocol was approved by the Institutional Animal Care and Use Committee of the Faculty of Science, Mahidol University, in accordance with the recommendations in the Guide for the Care and Use of Laboratory Animals of the US National Institutes of Health.

2.10. Mouse model of colitis-associated colorectal cancer

Male mice (20–25 g, C57/BL6 strain) were obtained from the National Laboratory Animal Center (Nakornpathom, Thailand). To induce CRC, mice received an intraperitoneal injection of azoxymethane (AOM; 7.5 mg/kg), followed by 2 cycles of 5-d exposure to 2.5% (w/v) dextran sulfate sodium (DSS; MW 36,000–50,000 Da; MP Biomedicals, Santa Ana, CA, USA) in drinking water starting on day 5 and day 26 after AOM injection, respectively [19]. COS was administered once daily on day 10 onward (after completion of the first cycle of 2.5% DSS) by orogastric gavage at 20 mg/kg, 100 mg/kg, or 500 mg/kg. Mice were then sacrificed on day 42 after AOM injection for histological and biomarker analyses. The experimental protocol was approved by the Institutional Animal Care and Use Committee of the Faculty of Science, Mahidol University, in accordance with the recommendations in the Guide for the Care and Use of Laboratory Animals of the US National Institutes of Health.

2.11. Data analysis and statistical procedures

Results are presented as means ± S.E.M. Statistical differences between control and treatment groups were evaluated using Student's *t* test, one-way ANOVA or two-way ANOVA followed by Bonferroni's post hoc test, where appropriate, with p value <0.05 being considered statistically significant.

3. Results

3.1. Effect of COS with different molecular weights on AMPK activation

Several biological activities of COS have been shown to depend on its molecular weight (MW) [16]. We therefore determined the effect of COS with different MW, i.e. 5,000 Da, 8,000 Da and 14,000 Da, on AMPK activation by performing Western blot

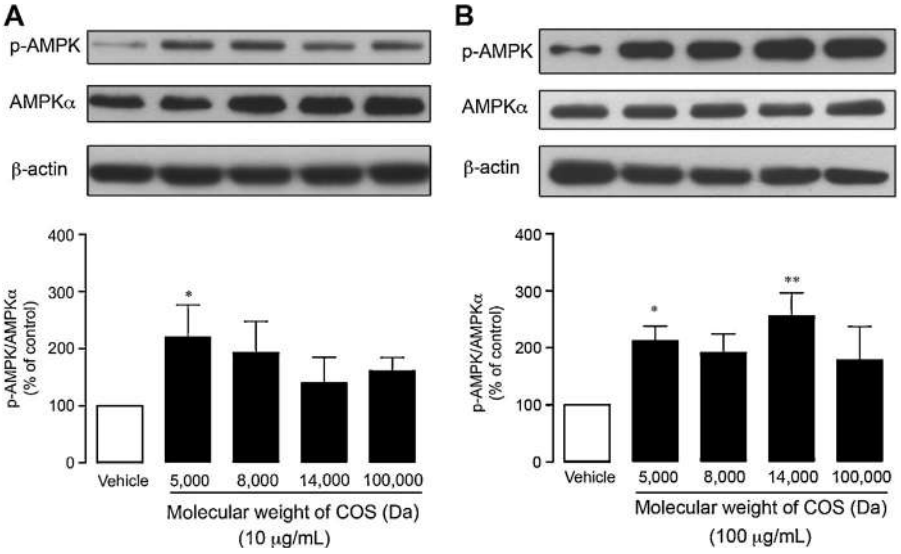

Fig. 1. Effects of COS with different averaged molecular weights on AMPK activation. Western blot analyses of p-AMPK, AMPKα, and β-actin after treating T84 cells with COS at (A) 10 μg/mL or (B) 100 μg/mL for one hour. Data are analyzed as the ratio of p-AMPK/AMPKα and expressed as % of control (vehicle-treated group), means ± S.E.M. (n = 5). $^{*}p < 0.05$; $^{**}p < 0.01$ compared with vehicle-treated group (one-way ANOVA).

analysis of the phosphorylated Thr-172 within the catalytic alpha subunit of AMPK (AMPKα). The effect of chitosan with MW of ~100,000 Da was also evaluated for comparison. T84 cell line was used in this study since it possesses physiological properties of IEC including barrier function regulation and chloride secretion. Treatment of T84 cells for an hour with chitosan or COS at 10 μg/mL resulted in increased AMPK phosphorylation. The highest and statistically significant degree of AMPK phosphorylation was observed with 5,000-Da COS (Fig. 1A). Similarly, treatments with 100 μg/mL of these compounds for an hour induced AMPK phosphorylation (Fig. 1B); however, only those with MW of 5,000 Da and 14,000 Da caused significant activation of AMPK. These results indicate that 5,000-Da COS has the highest potency in activating AMPK in T84 cells. Thereafter, COS with the averaged MW of 5,000 Da was selected for subsequent experiments to (1) characterize its AMPK-stimulating effects including cellular mechanisms and its impact on barrier function as well as NF-κB-mediated inflammatory responses in IEC, and (2) investigate its potential applications in the treatment of secretory diarrheas and CRC chemoprevention.

3.2. Characterization of AMPK activation by COS

To characterize the effect of COS in T84 cells, time course and dose-response of AMPK phosphorylation were investigated using Western blot analysis. In addition, phosphorylation of acetyl Co-A carboxylase (ACC) at Ser-79, a downstream target of AMPK, was determined using AICAR (1 mM), a known AMPK activator, as positive control. Results showed that COS (100 μg/mL) induced both AMPK phosphorylation and ACC phosphorylation in a time-dependent manner starting at 60 min post-treatment (Fig. 2A). Similarly, treatment with COS for 1 h resulted in AMPK activation in a concentration-dependent manner (Fig. 2B).

Furthermore, the effect of COS on AMPK phosphorylation was investigated in other IEC including HT-29 and Caco-2 cells. As shown in Fig. 2C, treatments with COS (10–500 μg/mL) for 24 h led to AMPK phosphorylation in a concentration-dependent manner. However, the dose that produced significant effects in these two cell lines was much higher, being 500 μg/mL compared to 100 μg/mL in T84 cells. In addition, it took longer time (24 h) to observe the effects in these cells. Therefore, only T84 cells were used in the subsequent experiments.

3.3. Involvement of CaMKKβ in mediating AMPK activation by COS

AMPK phosphorylation is mediated by two upstream kinases including LKB1 and CaMKKβ, which are sensitive to increased ADP:ATP ratio and increased $[Ca^{2+}]_i$, respectively [1]. Metformin (5 mM) was used as a positive control in this experiment. As depicted in Fig. 3A, 24-h treatment with COS (100 μg/mL) did not affect ADP:ATP ratio. This result indicates that the mechanism by which COS activates AMPK in T84 cells does not involve energy deprivation/change in ADP:ATP ratio. Next, the involvement of CaMKKβ in mediating COS-induced AMPK activation was investigated using CaMKKβ inhibitor STO-609. Interestingly, the effect of COS (100 μg/mL; 1-h treatment) on AMPK activation was significantly attenuated by pre-treatment with STO-609 (5 μM) (Fig. 3B). This result indicates that COS induces AMPK activation via CaMKKβ in T84 cells.

3.4. Effect of COS on intracellular calcium level

Since CaMKKβ-mediated AMPK activation is responsive to an increase in $[Ca^{2+}]_i$, the effect of COS on $[Ca^{2+}]_i$ was investigated using the ratiometric Ca^{2+} indicator indo-1. In this experiment, the ratio of emitted fluorescence at 405 nm (from Ca^{2+}-bound indo-1) to 490 nm (from Ca^{2+}-free indo-1) (indo-1 ratio) was used as an indicator of $[Ca^{2+}]_i$. As shown in Fig. 3C, an addition of COS (100 μg/mL) to T84 cells (extracellular $[Ca^{2+}]$ or $[Ca^{2+}]_o$ = 1 mM) caused an abrupt increase in indo-1 ratio, indicating that COS induces an increase in $[Ca^{2+}]_i$. To investigate the contribution of Ca^{2+} influx from extracellular source, effect of COS on $[Ca^{2+}]_i$ was investigated using Ca^{2+}-free buffer ($[Ca^{2+}]_o$ = 0 mM). Interestingly, the effect of COS (100 μg/mL) on $[Ca^{2+}]_i$ was unaffected by removal of $[Ca^{2+}]_o$ (Fig. 3C), indicating that an elevation of $[Ca^{2+}]_i$ induced by COS is due to Ca^{2+} release from intracellular sources.

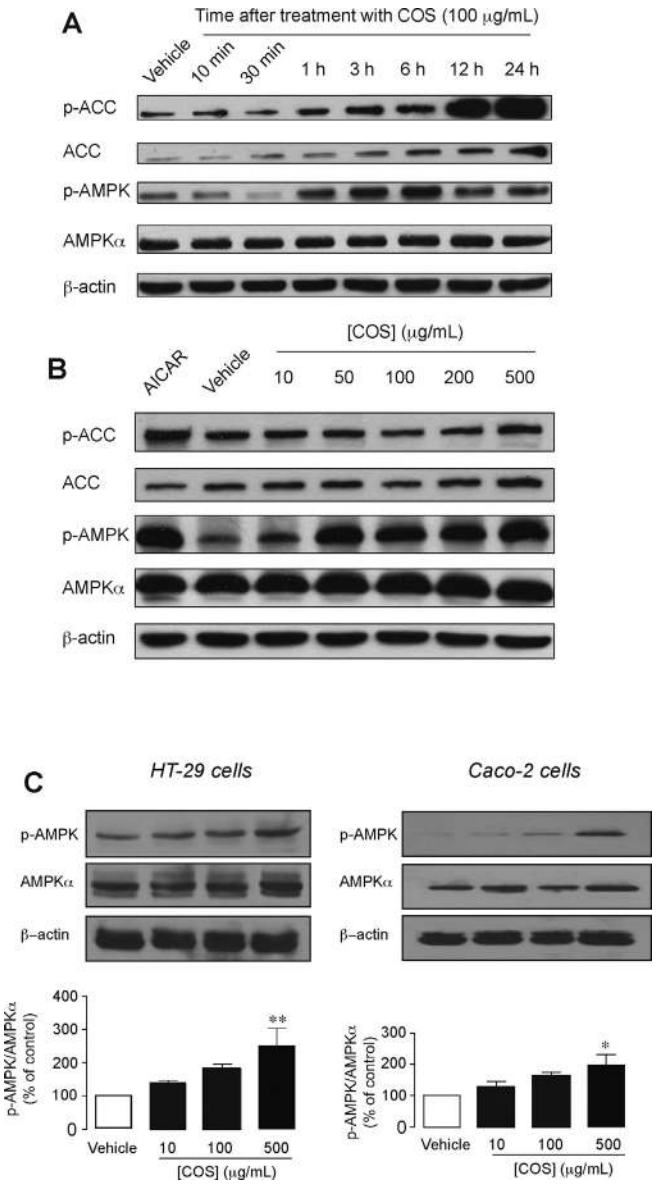

Fig. 2. Pharmacological characterization of the effects of COS (MW 5,000 Da) on the activation of AMPK and its downstream target. (A) Time course of AMPK activation and expression of p-ACC by COS. T84 cells were treated with vehicle or COS (100 μg/mL) for the indicated durations before sample collection for Western blot analysis. A representative immunoblot of three independent experiments is shown. (B) Dose-response of COS-induced AMPK activation and expression of p-ACC. T84 cells were incubated with AICAR, vehicle, or COS at the indicated concentrations for one hour before sample collection for Western blot analysis. A representative immunoblot of three independent experiments is shown. (C) Effects of COS on AMPK activation in HT-29 cells and Caco-2 cells. HT-29 cells and Caco-2 cells were treated with vehicle or COS at the indicated concentrations for 24 h before sample collection for Western blot analysis. Data are analyzed as the ratio of p-AMPK/AMPKα and expressed as % of control (vehicle-treated group), means ± S.E.M. (n = 4–6). $^{*}p < 0.05$; $^{**}p < 0.01$ compared with vehicle-treated group (one-way ANOVA).

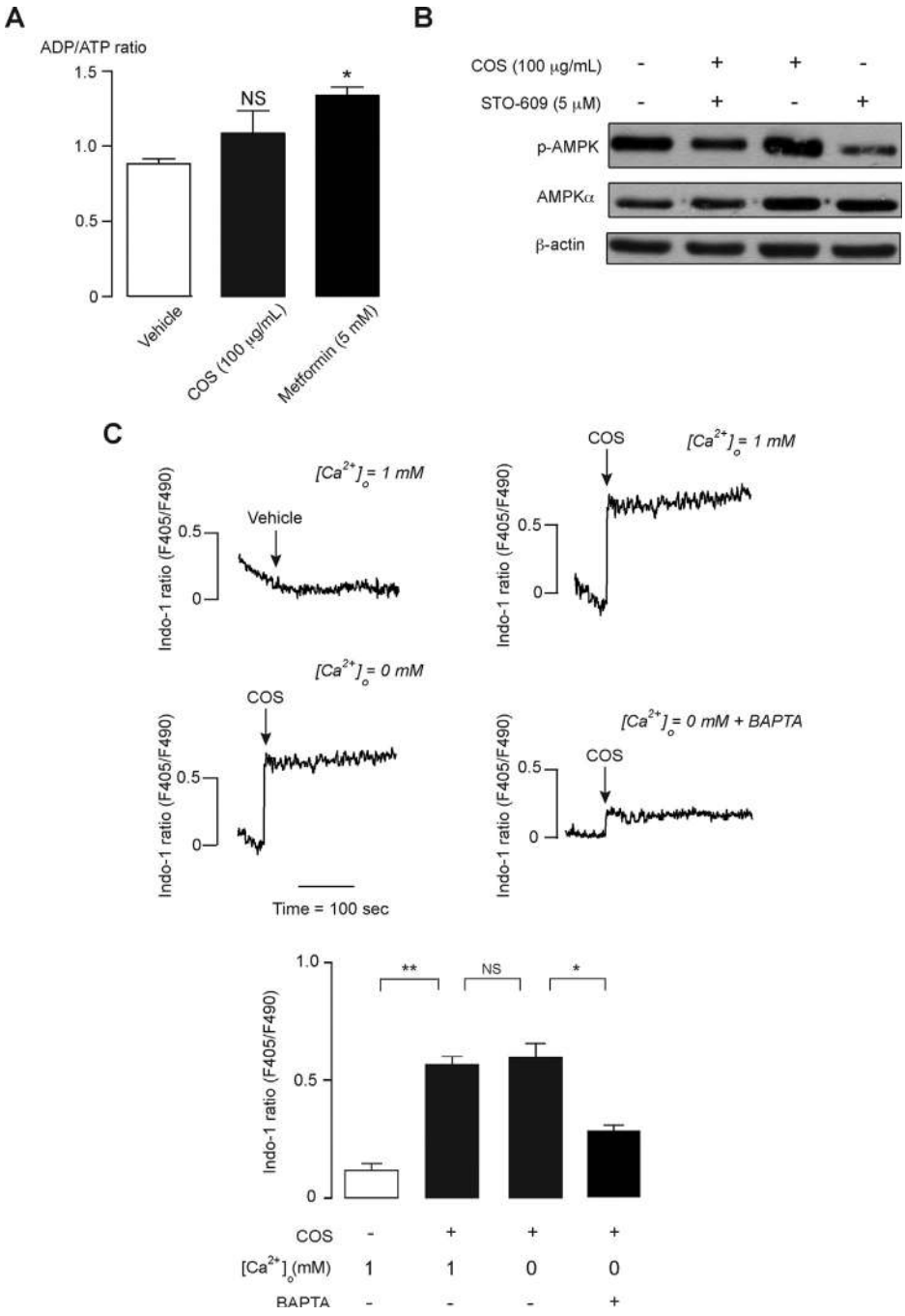

Fig. 3. Involvement of CaMKKβ in COS-induced AMPK activation and effect of COS on $[Ca^{2+}]_i$. (A) Effect of COS on ADP/ATP ratio. T84 cells were treated with vehicle, COS (100 μg/mL), or metformin (5 mM) for 24 h before measurements of ADP/ATP ratio. Data are expressed as means ± S.E.M. (n = 5) NS, non-significant; $^{*}p < 0.05$ compared with vehicle-treated group (one-way ANOVA). (B) Involvement of CaMKKβ in COS-induced AMPK activation. T84 cells were treated with COS (100 μg/mL) without or with CaMKKβ inhibitor STO-609 (5 μM) for 24 h before sample collection for Western blot analysis. A representative immunoblot of four independent experiments is shown. (C) Effect of COS on $[Ca^{2+}]_i$. After indo-1 loading, T84 cells were suspended in buffers supplemented with Ca^{2+} (1 mM) or without Ca^{2+} (with or without 0.2 mM BAPTA). During continual measurement of indo-1 dual fluorescence (emitted at 405 nm and 490 nm), vehicle or COS (100 μg/mL) was added into the bathing solutions. Top, representative tracings of indo-1 fluorescence ratio (F405/F490). Bottom, summary of the data is shown. Data are expressed as means of indo-1 fluorescence ratio (F405/F490) ± S.E.M. (n = 3–4). NS, non-significant; $^{*}p < 0.05$; $^{**}p < 0.01$ (Student's t test).

Of note, pretreatment with intracellular Ca^{2+} chelator BAPTA blunted the COS-induced increase in indo-1 ratio, confirming that COS elevates $[Ca^{2+}]_i$ (Fig. 3C).

3.5. Mechanism of COS-induced elevation in $[Ca^{2+}]_i$ and AMPK activation

Two main sources of intracellular Ca^{2+} are endoplasmic reticulum (ER) and mitochondria. Since the effect of COS on inducing elevation of $[Ca^{2+}]_i$ is rapid (~5–10 s after addition of COS), we hypothesized that COS may induce $[Ca^{2+}]_i$ release from ER via G-protein coupled receptor (G_q)-phospholipase C (PLC)-inositol triphosphate (IP_3) receptor-mediated pathway. Consistent with this hypothesis, pretreatment with thapsigargin (TG; 5 μM) and 2-aminoethoxydiphenyl borate (2-APB; 100 μM), which are inhibitors of Ca^{2+} ATPases and IP_3 receptor Ca^{2+} channels located on ER membrane, respectively, resulted in a significant decrease in COS-induced elevation of $[Ca^{2+}]_i$ (Fig. 4). This result indicates that COS induces Ca^{2+} release from ER. Furthermore, pretreatment with U73122 (PLC inhibitor; 10 μM)

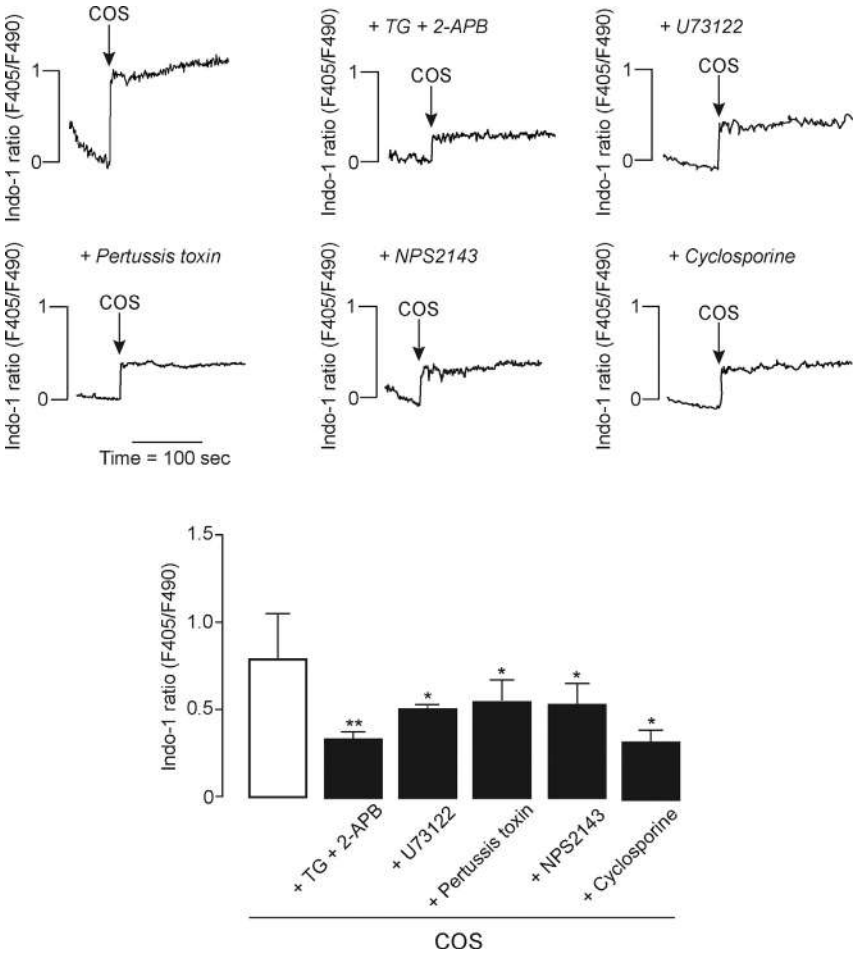

Fig. 4. Mechanism of COS-induced increases in $[Ca^{2+}]_i$. T84 cells were loaded with indo-1 and suspended in Ca^{2+}-free buffers. After the indicated pretreatments (5 μM TG + 100 μM 2-APB, 10 μM U73122, 2 μg/mL Pertussis toxin, 10 μM NPS2143, or 5 μM cyclosporine) for one hour, COS (100 μg/mL) was added into bathing solutions during continual recording of indo-1 dual fluorescence (emitted at 405 nm and 490 nm). Top, representative tracing of indo-1 fluorescence ratio (F405/F490). Bottom, summary of the data is shown. Data are expressed as means of indo-1 fluorescence ratio (F405/F490) ± S.E.M. (n = 3–6). $^{*}p < 0.05$; $^{**}p < 0.01$ compared with COS-treated control group (one-way ANOVA).

and Pertussis toxin (G protein inhibitor; 2 μg/mL) significantly suppressed COS-induced $[Ca^{2+}]_i$ elevation (Fig. 4), suggesting that COS induces Ca^{2+} release from ER via G_q-PLC-dependent pathway.

It is known that calcium-sensing receptor (CaSR), a G_q-coupled receptor linked to PLC, is expressed in IEC including T84 cells [20]. In addition, several cationic nitrogen-containing molecules including aminoglycosides (e.g. neomycin and gentamicin), polyamines (e.g. spermine), and aromatic L-amino acid (e.g. L-phenylalanine) have been shown to act as CaSR agonist [21]. This led us to hypothesize that COS, which exists as a cationic molecule at physiological pH, may increase $[Ca^{2+}]_i$ in T84 cells by activating CaSR. In support of this hypothesis, pretreatment with a selective CaSR antagonist NPS2143 (10 μM) significantly suppressed a COS-induced increase in $[Ca^{2+}]_i$ (Fig. 4). Since increased $[Ca^{2+}]_i$ is known to trigger Ca^{2+} release from mitochondria via mitochondrial permeability transition pore (MPTP), the contribution of the Ca^{2+} release from mitochondria to COS-induced increases in $[Ca^{2+}]_i$ was investigated using cyclosporine, an MPTP inhibitor. Interestingly, cyclosporine pretreatment (5 μM) significantly reduced COS-induced $[Ca^{2+}]_i$ elevation (Fig. 4). Our results, therefore, indicate that COS induces Ca^{2+} release from both ER and mitochondria, at least in part, via CaSR-PLC-IP_3 receptor channel-dependent pathway.

Next, the contribution of COS-induced $[Ca^{2+}]_i$ elevation to the AMPK activation was investigated. As shown in Fig. 5, COS-induced AMPK phosphorylation was significantly suppressed by pretreatments with BAPTA, TG plus 2-APB, U73122, Pertussis toxin, NPS2143, and cyclosporine. These results strongly suggest that COS activates AMPK by inducing Ca^{2+} release from ER and mitochondria, at least in part, via CaSR-PLC-IP_3 receptor-dependent pathway.

3.6. COS promotes tight junction assembly via AMPK-dependent mechanism

AMPK is known to facilitate extracellular Ca^{2+}-induced tight junction assembly in epithelial cells [5,6]. We next determined the effect of COS on the extracellular Ca^{2+}-induced tight junction assembly in T84 cell monolayers using Ca^{2+} switch assay. As depicted in Fig. 6A, treatment with COS (100 μg/mL) led to a significant increase in TEER at 24 h post-treatment compared with control. Furthermore, this effect was inhibited by pretreatment with compound C (80 μM), an AMPK inhibitor. Of note, the effect of COS on TEER was absent without Ca^{2+} re-addition, i.e. in Ca^{2+}-free condition (Fig. 6B). These findings indicate that extracellular Ca^{2+}-induced tight junction assembly was enhanced by COS via the AMPK-dependent pathway.

3.7. Suppression of NF-κB-mediated inflammatory response by COS is independent of AMPK

Our previous study showed that COS inhibited NF-κB activation in IEC, leading to amelioration of intestinal inflammation in mouse

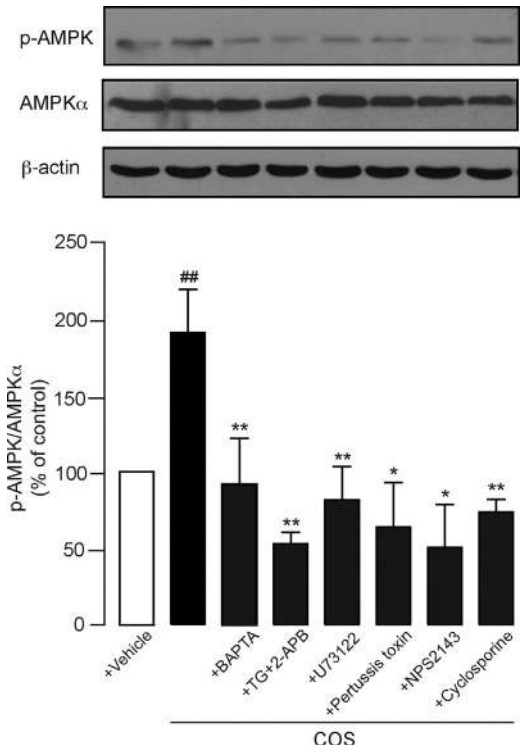

Fig. 5. Mechanism of COS-induced AMPK activation. T84 cells were pretreated for one hour with the indicated compounds (0.2 mM BAPTA, 5 μM TG + 100 μM 2-APB, 10 μM U73122, 2 μg/mL Pertussis toxin, 10 μM NPS2143, or 5 μM cyclosporine), then incubated for 24 h with COS (100 μg/mL), after which proteins were collected for Western blot analysis. Top, a representative immunoblot from five independent experiments is shown. Bottom, summary of the data. Data are analyzed as the ratio of p-AMPK/AMPKα and expressed as % of control (COS-untreated group), means ± S.E.M. ($n = 5$). $^{*}p < 0.05$; $^{**}p < 0.01$ compared with COS-treated control group. $^{\#\#}p < 0.01$ compared with no treatment (one-way ANOVA).

models of IBD [18]. We, therefore, investigated the involvement of AMPK in COS-induced suppression of NF-κB-transcriptional activity and NF-κB-mediated inflammatory responses. In this experiment, TNFα (10 ηg/mL) was used as an inducer of NF-κB signaling. We investigated the effect of COS on NF-κB transcriptional activity using T84 cells transfected with NF-κB-GFP fusion plasmid and analyzed the indicators of NF-κB activation in IEC such as epithelial barrier disruption and protein expressions of inflammatory mediators including inducible nitric oxide synthase (iNOS) and cyclooxygenase-2 (COX-2). As illustrated in Fig. 7A, COS (100 μg/mL) significantly suppressed TNFα-induced NF-κB promoter activity and this effect was not reversed by pretreatment with compound C (80 μM). Consistent with this result, COS (100 μg/mL) inhibited protein expressions of NF-κB target genes including iNOS and COX-2 in an AMPK-independent manner (Fig. 7B). In addition, COS (100 μg/mL) prevented TNFα-induced FITC-dextran flux, an indicator of intestinal epithelial barrier disruption, across T84 cell monolayers. Likewise, this effect was not reversed by pretreatment with compound C (Fig. 7C). Therefore, our data indicate that COS-induced inhibition of NF-κB signaling is not mediated by AMPK in T84 cells.

3.8. Potential applications of COS in the treatment of secretory diarrhea and chemoprevention of colorectal cancer

We next investigated an *in vivo* efficacy of COS in activating AMPK in intestinal tissues and in the treatment of secretory diarrheas and chemoprevention of CRC in mice. Anti-secretory efficacy of COS was evaluated in a mouse closed loop model of cholera toxin (CT)-induced intestinal fluid secretion. As shown in Fig. 8A, treatment with COS (100 μg/mL) reduced CT-induced intestinal fluid secretion by ~30%. In addition, mice receiving COS showed increased phosphorylation of AMPK and ACC in their intestinal tissues (Fig. 8B), confirming that COS activates AMPK in mouse intestine *in vivo*.

The chemopreventive efficacy of COS was investigated in a mouse model of colitis-associated CRC, in which mice received intraperitoneal injection of AOM and 2.5% DSS in drinking water. Over the entire period of the experiment, body weights and food consumption of CRC mice with/without treatment with COS were not different from those of the control healthy mice (data not shown). Of particular interest, the number of aberrant crypt foci (ACF), premalignant biomarkers of CRC, in the colon specimens was significantly reduced by treatment with COS at 500 mg/kg (Fig. 9 A and B). To gain insight into the mechanisms of chemopreventive efficacy of COS, Western blot analysis of the colon samples was performed. As shown in Fig. 10A and B, significant increases of AMPK and ACC phosphorylation were observed in mice treated with 500 mg/kg COS. In addition, the effect of COS on the expression of β-catenin, a molecular biomarker of CRC development, was investigated. Fig. 10C shows that COS induced a dose-dependent reduction in β-catenin expression in mouse colon with a significant effect at the dose of 500 mg/kg. Since AMPK activation has been shown to exert a chemopreventive effect, in part, by inducing apoptosis of premalignant cells, the expression of cleaved caspase-3 was, therefore, investigated in the colon samples. Results show that mice receiving COS exhibited an increase in the level of cleaved caspase-3 expression in a dose-dependent manner with a significant effect at the dose of 500 mg/kg COS (Fig. 10D).

4. Discussion

Chitosan oligosaccharides (COS), which are natural oligomers derived from chitin, are the most abundant carbohydrate polymers second to cellulose. Despite being employed as food supplements with a variety of claimed actions, the cellular/molecular mechanisms underlying their biological activities/benefits are poorly understood. In this study, we demonstrated the novel effect of COS in activating AMPK via mechanisms involving CaSR-PLC-mediated Ca^{2+} release from ER in IEC. AMPK activation by COS led to facilitation of tight junction assembly in IEC. Of particular importance, this report showed that ingestion of COS induced AMPK activation in intestinal tissues *in vivo* and inhibited intestinal fluid secretion in secretory diarrheas and premalignant development of CRC in mice.

This study identified the unprecedented action of COS in activating AMPK in an epithelial cell line. In fact, AMPK has recently been shown to play many pivotal roles in regulating epithelial functions including facilitation of tight junction assembly and inhibition of CFTR-mediated chloride secretion [4,7]. In addition, several studies have shown that some known drugs such as aspirin and fenamates activate AMPK, which may account for the anti-inflammatory and chemopreventive effects of these drugs [22,23]. In the present study, COS with the averaged MW of 5,000 Da had more pronounced AMPK-stimulating effect than those with higher MW (8,000 Da, 14,000 Da and 100,000 Da). This finding is in agreement with other investigations demonstrating that low MW COS has more favorable biological activities including higher anti-inflammatory effects, in addition to its lower toxicity and higher biocompatibility [24]. Furthermore, we found that activation of AMPK was initially observed at 1-h post-treatment and sustained for 24 hours. Interestingly, the effect of COS was observed in other human IEC lines including HT-29 and Caco-2 cells, indicating that this effect is not cell-line specific. In light of

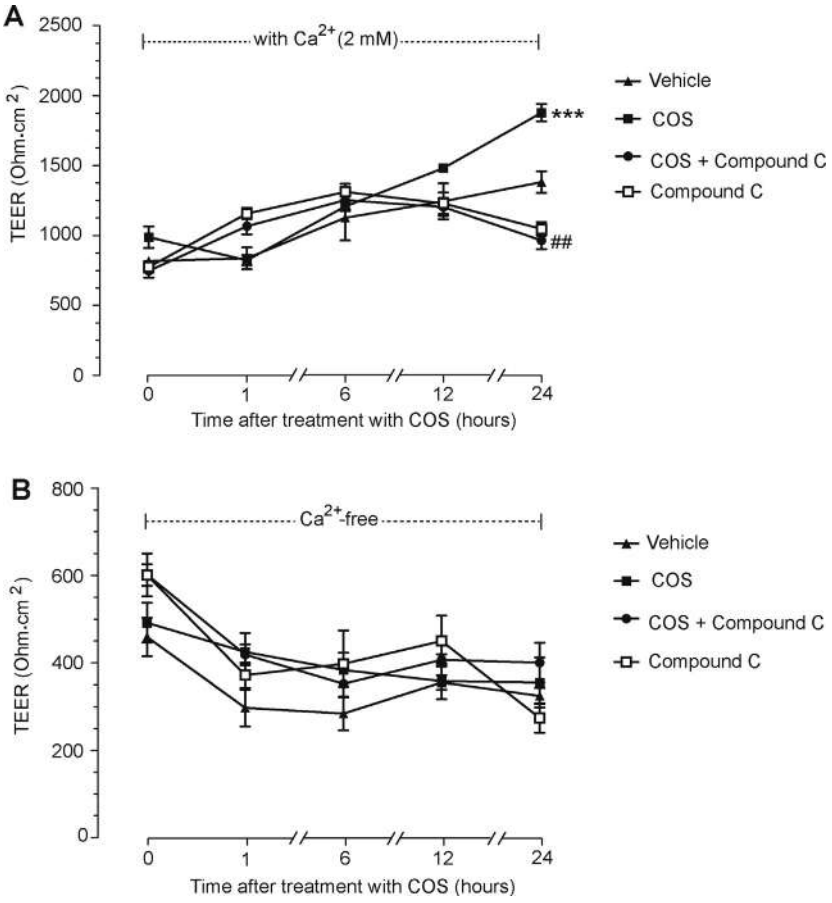

Fig. 6. Effect of COS on tight junction assembly. (A) Effect of COS on tight junction assembly using Ca^{2+} switch assay, T84 cells were cultured for 16 hours in Ca^{2+}-free media. TEER of T84 cell monolayers was then measured after replacement of Ca^{2+}-free media with media containing Ca^{2+} (2 mM) and the indicated reagents (COS at 100 μg/mL; compound C at 80 μM). Data are expressed as means of TEER ± S.E.M. ($n = 6$). $^{***}p < 0.001$ compared with vehicle-treated group. $^{\#\#}p < 0.01$ compared with COS-treated group (one-way ANOVA). (B) Effect of COS on tight junction assembly in Ca^{2+}-free media. T84 cell monolayers were cultured for 16 h in Ca^{2+}-free media. TEER was then measured after addition of the indicated compounds into the culture media (COS at 100 μg/mL; compound C at 80 μM). Data are expressed as means of TEER ± S.E.M. ($n = 6$)(two-way ANOVA, Treatment and Time).

the data obtained from this study, we proposed that COS activates AMPK activity in T84 cells mainly by inducing $[Ca^{2+}]_i$ elevation since (1) COS had no effect on ADP/ATP ratio, the primary stimulus of LKB1-mediated AMPK activation, (2) CaMKKβ inhibitor STO-609 and intracellular Ca^{2+} chelator BAPTA completely abrogated COS-induced AMPK activation, and (3) COS induced an abrupt increase in $[Ca^{2+}]_i$. Using a variety of pharmacological inhibitors, our results indicate that COS increases $[Ca^{2+}]_i$ and activates AMPK, at least in part, via CaSR-G_q-PLC-IP_3-receptor channel-dependent pathway. In fact, CaSR agonists have previously been shown to elevate $[Ca^{2+}]_i$ in IEC via G_q-PLC-IP_3 receptor channel pathway [20]. Similar to the known CaSR agonists including neomycin and gentamicin, COS consists of cationic N-containing carbohydrate molecules [21]. Therefore, we speculate that COS may increase $[Ca^{2+}]_i$ by interacting with CaSR, subsequently eliciting Ca^{2+} release from ER. However, to gain more insight into the interaction between COS and CaSR, future studies are required. Furthermore, our study indicates that Ca^{2+} release from mitochondria via MPTP may also be involved in $[Ca^{2+}]_i$ elevation and AMPK activation in IEC. This observation is consistent with the factual knowledge that $[Ca^{2+}]_i$ is tightly regulated by both ER and mitochondria and these two organelles are functionally interconnected [25].

In this study, COS enhanced tight junction assembly in T84 cell monolayers in an AMPK- and extracellular Ca^{2+}- dependent manner. Indeed, the roles of CaSR and AMPK in mediating extracellular Ca^{2+}-induced tight junction assembly have previously been demonstrated in Madin-Darby canine kidney (MDCK) cell monolayers [5,6,26]. Interestingly, we found that the enhancement of tight junction assembly was absent in Ca^{2+}-free media. This observation is in line with the previous studies demonstrating that AMPK activator AICAR failed to induce maturation of tight junction formation in low Ca^{2+} media [5,6]. Previously, we have shown that COS (MW of 5,000 Da) ameliorates intestinal inflammation and the associated morbidity and mortality in the two mouse models of colitis via suppression of NF-κB-mediated inflammatory response and barrier disruption [18]. Although AMPK is known to be a negative regulator of NF-κB signaling [27], our data in the present study showed that the inhibitory effect of COS on NF-κB signaling and the associated tight junction disruption were not reversed by AMPK inhibitor compound C. This suggests that COS may suppress NF-κB-mediated inflammatory responses and prevent the inflammation-associated barrier disruption in IEC via an AMPK-independent mechanism, which warrants further investigations.

AMPK has been implicated as a drug target for reducing intestinal fluid loss in secretory diarrheas especially cholera, and for chemoprevention of CRC [9,14]. In a mouse model of CT-induced fluid secretion, we demonstrated that COS effectively prevented CT-induced intestinal fluid secretion. Western blot analyses of phosphorylated AMPK and ACC confirmed that COS activated AMPK in intestinal tissues *in vivo*. Furthermore, oral administration of COS reduced the numbers of ACF, the premalignant markers of CRC, in a mouse model of colitis-associated

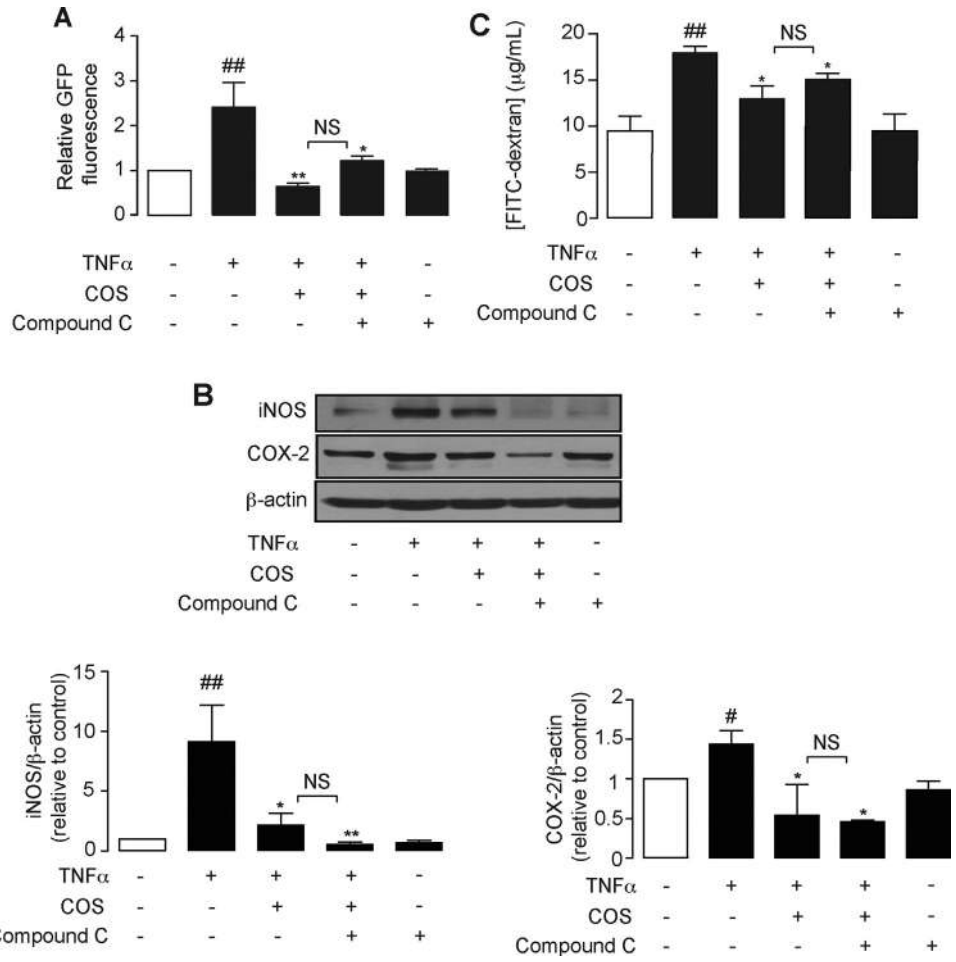

Fig. 7. COS-induced suppression of NF-κB-mediated inflammatory response and barrier disruption is AMPK-independent. (A) Effect COS on NF-κB transcriptional activity. T84 cells were transfected with NF-κB-GFP fusion plasmid and subjected to the indicated treatments (10 ηg/mL TNFα, 100 μg/mL COS, 80 μM compound C). GFP fluorescence intensity was measured using flow cytometer. Data are expressed as means of relative GFP fluorescence intensity ± S.E.M. (n = 8). NS, non-significant. $^{*}p < 0.05$; $^{**}p < 0.01$ compared with the group treated with TNFα alone. $^{\#\#}p < 0.01$ compared with group with no treatment (one-way ANOVA). (B) Effect of COS on TNFα-induced expression of inflammatory markers. After 24-h treatment of T84 cells with the indicated reagents, samples were collected for immunoblot analysis of iNOS and COX-2. Top, representative immunoblot. Bottom, summary of the data. Data are expressed as means of relative band intensity of iNOS or COX-2 normalized by β-actin ± S.E.M. (n = 6). NS, non-significant. $^{*}p < 0.05$; $^{**}p < 0.01$ compared with TNF-α alone. $^{\#}p < 0.05$; $^{\#\#}p < 0.01$ compared with no treatment (one-way ANOVA). (C) Effect of COS on TNFα-induced barrier disruption. T84 cell monolayers were exposed for 24 hours to the indicated treatments before FITC-dextran (4.4 kDa) flux assays. Data are expressed as means of FITC-dextran concentration ± S.E.M. (n = 6). NS, non-significant. $^{*}p < 0.05$ compared with TNFα alone. $^{\#\#}p < 0.01$ compared with no treatment (one-way ANOVA).

tumorigenesis. Of note, the suppressive effect of COS on ACF numbers was significant at the dose of 500 mg/kg, which is well correlated with the effects on activation of AMPK phosphorylation, suppression of β-catenin expression and induction of cleaved caspase-3 expression in intestinal tissues. This correlation suggests that COS at 500 mg/kg is required to provide effective chemoprevention against CRC and that the chemopreventive effect of COS is mediated at least in part via AMPK activation. This dose of COS in mice can be translated to 40 mg/kg for human based on body surface areas of humans and mice [28].

In addition to their potential benefits in secretory diarrheas and CRC, agents possessing AMPK-stimulating activity have been proposed to hold promise in the treatment of several other diseases. For example, AMPK activation by both known drugs (e.g. metformin and aspirin) and natural compounds (e.g. resveratrol and berberine) has been shown to ameliorate metabolic syndrome-associated disorders including type II diabetes mellitus, hypertension, dyslipidemia, atherosclerosis and Alzheimer's disease [29–34]. Importantly, AMPK activators such as aspirin, metformin and resveratrol have been shown to have potential in extending lifespan of organisms by activating sirtuins, a group of histone/protein deacetylases involved in combating aging [35–37]. Indeed, ingestion of COS has previously been shown to exert anti-diabetic effects in type II diabetic rats by improving insulin sensitivity and increasing insulin secretion from pancreatic β cells [38,39]. In addition, COS has been found to be effective in improving plasma lipid profiles in mice and alleviating β-amyloid peptide-induced toxicity in rat primary hippocampal neurons [40]. However, the involvement of AMPK in eliciting these beneficial effects of COS has not yet been investigated and represents important issues for future investigations.

In conclusion, COS induces AMPK activation in IEC, at least in part, via a mechanism involving CaSR-PLC-IP_3 receptor channel-mediated elevation in $[Ca^{2+}]_i$. Activation of AMPK then promotes tight junction assembly and leads to suppression of CFTR-mediated intestinal fluid secretion and chemoprevention of CRC *in vivo*. This study not only provides a rational basis for potential utility of COS in the treatment of secretory diarrheas and chemoprevention of CRC, but also constitutes a novel body of knowledge regarding mechanisms underlying the beneficial effects of COS.

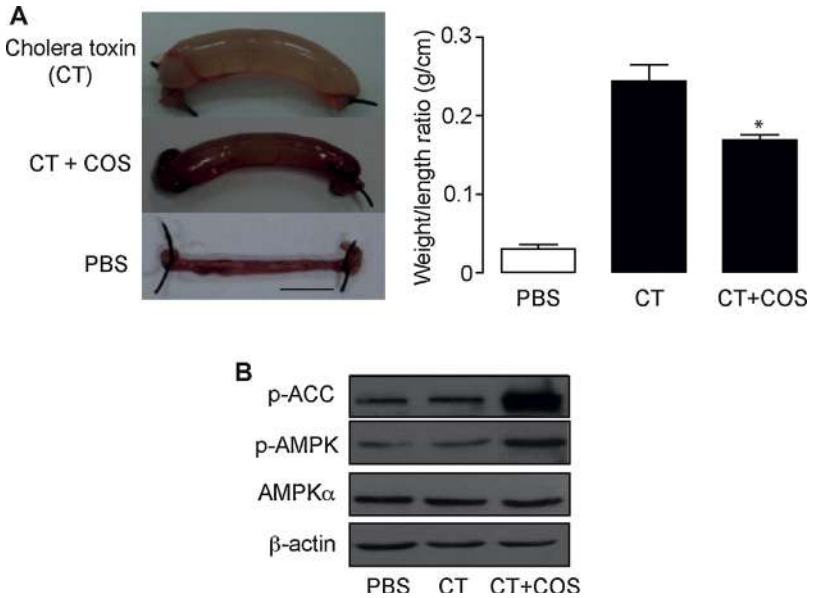

Fig. 8. Anti-diarrheal efficacy of COS in a mouse closed loop model of cholera. Ileal loops were instilled with cholera toxin (CT, 1 μg), CT (1 μg) plus COS (100 μg/mL) or PBS alone. Four hours thereafter, ileal loops were removed for measuring loop weight/length ratio and the ileal tissues were collected for Western blot analysis. (A) Effect of COS on CT-induced intestinal fluid secretion. Left, photographs of representative ileal loops. Scale bar = 1 cm. Right, summary of the data. Data are expressed as means of loop weight/length ratio ± S.E.M. ($n = 5$). $^{*}p < 0.05$ compared with CT-treated group (Student's t test). (B) COS-induced AMPK activation in ileal loops. Expressions of p-ACC, p-AMPK, AMPKα, and β-actin were determined using Western blot analysis. A representative immunoblot from five mice is shown.

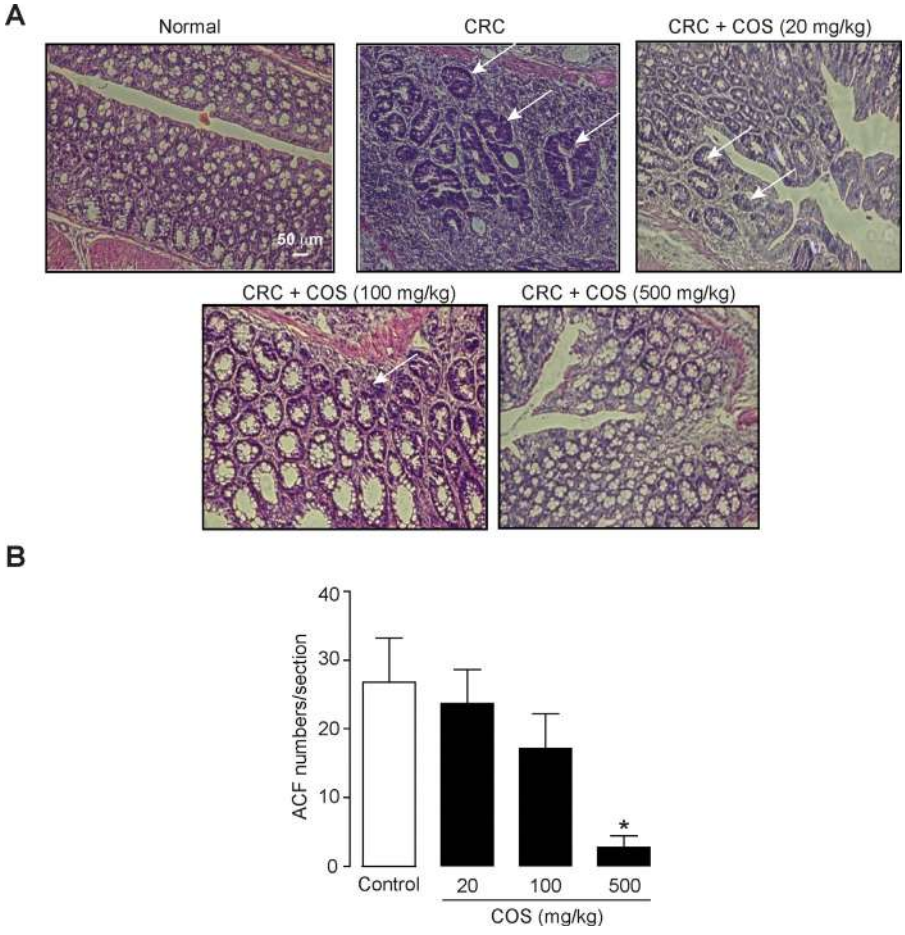

Fig. 9. Chemopreventive efficacy of COS against CRC in mice. A mouse model of colitis-associated carcinogenesis was induced by an intraperitoneal administration of azoxymethane (7.5 mg/kg BW) followed by two cycles of 5-d exposure to dextran sulfate sodium (DSS, 2.5%, w/v) in drinking water. Vehicle (control) or COS at the indicated doses was intragastrically administered to the mice once a day after completion of the first cycle of 2.5% DSS. (A) Representative micrographs of colon tissues stained with hematoxylin and eosin (100× magnification). Arrows indicate aberrant crypt foci (ACF). Scale bar = 50 μm. (B) Effect of COS administration on ACF numbers. Data are expressed as means of ACF numbers/section ± S.E.M. ($n = 9$). $^{*}p < 0.05$ compared with vehicle-treated mice (control) (one-way ANOVA).

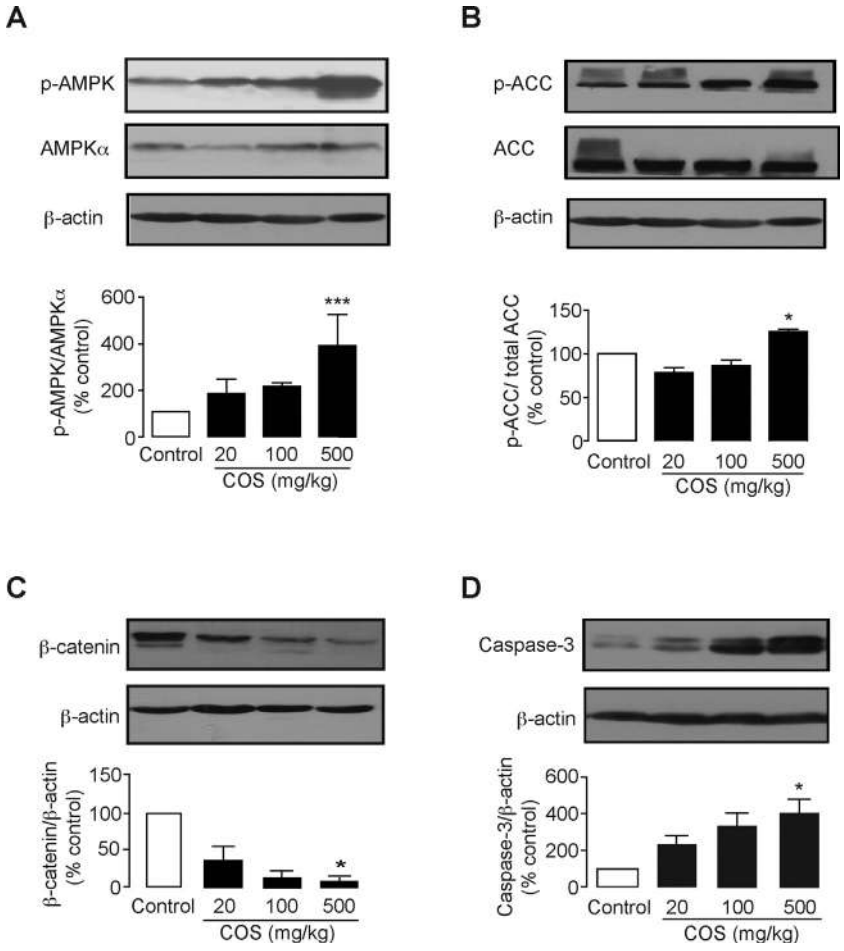

Fig. 10. Effect of COS administration on the expression of cancer-related biomarkers in a mouse model of colitis-associated CRC. (A) AMPK phosphorylation. (B) ACC phosphorylation. (C) β-catenin expression. (D) Cleaved caspase-3 expression. Data are expressed as means of relative band intensity normalized by total non-phosphorylated forms of proteins or β-actin ± S.E.M. ($n = 6$). $^{*}p < 0.05$; $^{***}p < 0.001$ compared with vehicle-treated group (control) (one-way ANOVA).

Acknowledgements

This work is supported by grants from the Agricultural Research Development Agency (ARDA), Thailand Research Fund (TRF) and Mahidol University (grant RSA5680006), and National Research Council of Thailand (NRCT) (to C.M.). Financial supports from the Faculty of Science, Mahidol University, and the Office of the Higher Education Commission and Mahidol University under the National Research Universities Initiative are also gratefully acknowledged (to C.M.). C.M. is TRF Research Scholar. SS is supported by TRF through the Royal Golden Jubilee Ph.D. Program (Grant PHD/0105/2556). Authors thank Professor Chumpol Prolpramool for critical reading of the manuscript.

References

[1] D.G. Hardie, M.L. Ashford, AMPK: regulating energy balance at the cellular and whole body levels, Physiology (Bethesda) 29 (2014) 99–107.
[2] K.R. Hallows, P.F. Mount, N.M. Pastor-Soler, Power DA. Role of the energy sensor AMP-activated protein kinase in renal physiology and disease, Am. J. Physiol. Renal. Physiol. 298 (2010) F1067–F1077.
[3] T. Yano, T. Matsui, A. Tamura, M. Uji, S. Tsukita, The association of microtubules with tight junctions is promoted by cingulin phosphorylation by AMPK, J. Cell Biol. 203 (2013) 605–614.
[4] M.J. Caplan, P. Seo-Mayer, L. Zhang, Epithelial junctions and polarity complexes and kinases, Curr. Opin. Nephrol. Hyperten. 17 (2008) 506–512.
[5] B. Zheng, L.C. Cantley, Regulation of epithelial tight junction assembly and disassembly by AMP-activated protein kinase, Proc. Natl. Acad. Sci. U.S.A. 104 (2007) 819–822.
[6] L. Zhang, J. Li, L.H. Young, M.J. Caplan, AMP-activated protein kinase regulates the assembly of epithelial tight junctions, Proc. Natl. Acad. Sci. U.S.A. 103 (2006) 17272–17277.
[7] J.D. King Jr., A.C. Fitch, J.K. Lee, J.E. McCane, D.O. Mak, J.K. Foskett, et al., AMP-activated protein kinase phosphorylation of the R domain inhibits PKA stimulation of CFTR, Am. J. Physiol. Cell Physiol. 297 (2009) C94–C101.
[8] C. Muanprasat, V. Chatsudthipong, Cholera pathophysiology and emerging therapeutic targets, Future Med. Chem. 5 (2013) 781–798.
[9] A.C. Rogers, L. Huetter, N. Hoekstra, D. Collins, A. Collaco, A.W. Baird, et al., Activation of AMPK inhibits cholera toxin stimulated chloride secretion in human and murine intestine, PloS One 8 (2013) e69050.
[10] R.Y. Su, Y. Chao, T.Y. Chen, D.Y. Huang, W.W. Lin, 5-Aminoimidazole-4-carboxamide riboside sensitizes TRAIL- and TNF{alpha}-induced cytotoxicity in colon cancer cells through AMP-activated protein kinase signaling, Mol. Cancer Therap. 6 (2007) 1562–1571.
[11] W. Li, B. Hua, S.M. Saud, H. Lin, W. Hou, M.S. Matter, et al., Berberine regulates AMP-activated protein kinase signaling pathways and inhibits colon tumorigenesis in mice, Mol. Carcinog. (2014).
[12] S.J. Koh, J.M. Kim, I.K. Kim, S.H. Ko, J.S. Kim, Anti-inflammatory mechanism of metformin and its effects in intestinal inflammation and colitis-associated colon cancer, J. Gastroenterol. Hepatol. 29 (2014) 502–510.
[13] E. Zulato, F. Bergamo, A. De Paoli, G. Griguolo, G. Esposito, G.L. De Salvo, et al., Prognostic significance of AMPK activation in advanced stage colorectal cancer treated with chemotherapy plus bevacizumab, Br. J. Cancer 111 (2014) 25–32.
[14] M.A. Anwar, W.A. Kheir, S. Eid, J. Fares, X. Liu, A.H. Eid, et al., Colorectal and prostate cancer risk in diabetes: metformin, an actor behind the scene, J. Cancer 5 (2014) 736–744.
[15] N. Thadathil, S.P. Velappan, Recent developments in chitosanase research and its biotechnological applications: a review, Food Chem. 150 (2014) 392–399.
[16] G. Lodhi, Y.S. Kim, J.W. Hwang, S.K. Kim, Y.J. Jeon, J.Y. Je, et al., Chitooligosaccharide and its derivatives preparation and biological applications, BioMed Res. Int. 2014 (2014) 654913.
[17] J.Y. Je, S.K. Kim, Chitooligosaccharides as potential nutraceuticals: production and bioactivities, Adv. Food Nutrit. Res. 65 (2012) 321–336.

[18] M. Yousef, R. Pichyangkura, S. Soodvilai, V. Chatsudthipong, C. Muanprasat, Chitosan oligosaccharide as potential therapy of inflammatory bowel disease: therapeutic efficacy and possible mechanisms of action, Pharmacol. Res. 66 (2012) 66–79.
[19] S. Huber, N. Gagliani, L.A. Zenewicz, F.J. Huber, L. Bosurgi, B. Hu, et al., IL-22BP is regulated by the inflammasome and modulates tumorigenesis in the intestine, Nature 491 (2012) 259–263.
[20] L. Gama, L.M. Baxendale-Cox, G.E. Breitwieser, Ca2+-sensing receptors in intestinal epithelium, Am. J. Physiol. 273 (1997) C1168–C1175.
[21] Z. Saidak, M. Brazier, S. Kamel, R. Mentaverri, Agonists and allosteric modulators of the calcium-sensing receptor and their therapeutic applications, Mol. Pharmacol. 76 (2009) 1131–1144.
[22] S.A. Hawley, M.D. Fullerton, F.A. Ross, J.D. Schertzer, C. Chevtzoff, K.J. Walker, et al., The ancient drug salicylate directly activates AMP-activated protein kinase, Science 336 (2012) 918–922.
[23] Y. Chi, K. Li, Q. Yan, S. Koizumi, L. Shi, S. Takahashi, et al., Nonsteroidal anti-inflammatory drug flufenamic acid is a potent activator of AMP-activated protein kinase, J. Pharmacol Exp. Therap. 339 (2011) 257–266.
[24] S.H. Lee, M. Senevirathne, C.B. Ahn, S.K. Kim, J.Y. Je, Factors affecting anti-inflammatory effect of chitooligosaccharides in lipopolysaccharides-induced RAW264.7 macrophage cells, Bioorg. Med. Chem. Lett. 19 (2009) 6655–6658.
[25] S. Marchi, S. Patergnani, P. Pinton, The endoplasmic reticulum-mitochondria connection: one touch, multiple functions, Biochim. Biophys. Acta 2014 (1837) 461–469.
[26] F. Jouret, J. Wu, M. Hull, V. Rajendran, B. Mayr, C. Schofl, et al., Activation of the Ca(2)+-sensing receptor induces deposition of tight junction components to the epithelial cell plasma membrane, J. Cell Sci. 126 (2013) 5132–5142.
[27] A. Salminen, J.M. Hyttinen, K. Kaarniranta, AMP-activated protein kinase inhibits NF-kappaB signaling and inflammation: impact on healthspan and lifespan, J. Mol. Med. (Berl.) 89 (2011) 667–676.
[28] S. Reagan-Shaw, M. Nihal, N. Ahmad, Dose translation from animal to human studies revisited, FASEB J. Off. Public. Feder. Am. Soc. Exp. Biol. 22 (2008) 659–661.
[29] T. Szkudelski, K. Szkudelska, Resveratrol and diabetes: from animal to human studies, Biochim. Biophys. Acta (2014).
[30] G.J. Gowans, D.G. Hardie, AMPK a cellular energy sensor primarily regulated by AMP, Biochem. Soc. Trans. 42 (2014) 71–75.
[31] T.A. Almabrouk, M.A. Ewart, I.P. Salt, S. Kennedy, Perivascular fat, AMP-activated protein kinase and vascular diseases, Br. J. Pharmacol. 171 (2014) 595–617.
[32] I. Pernicova, M. Korbonits, Metformin–mode of action and clinical implications for diabetes and cancer, Nature Rev. Endocrinol. 10 (2014) 143–156.
[33] V. Vingtdeux, L. Giliberto, H. Zhao, P. Chandakkar, Q. Wu, J.E. Simon, et al., AMP-activated protein kinase signaling activation by resveratrol modulates amyloid-beta peptide metabolism, J. Biol. Chem. 285 (2010) 9100–9113.
[34] X. Fan, J. Wang, J. Hou, C. Lin, A. Bensoussan, D. Chang, et al., Berberine alleviates ox-LDL induced inflammatory factors by up-regulation of autophagy via AMPK/mTOR signaling pathway, J. Trans. Med. 13 (2015) 450.
[35] A. Martin-Montalvo, E.M. Mercken, S.J. Mitchell, H.H. Palacios, P.L. Mote, M. Scheibye-Knudsen, et al., Metformin improves healthspan and lifespan in mice, Nature Commun. 4 (2013) 2192.
[36] N.L. Price, A.P. Gomes, A.J. Ling, F.V. Duarte, A. Martin-Montalvo, B.J. North, et al., SIRT1 is required for AMPK activation and the beneficial effects of resveratrol on mitochondrial function, Cell Metab. 15 (2012) 675–690.
[37] S. Ayyadevara, P. Bharill, A. Dandapat, C. Hu, M. Khaidakov, S. Mitra, et al., Aspirin inhibits oxidant stress, reduces age-associated functional declines, and extends lifespan of Caenorhabditis elegans, Antioxid. Redox Signal. 18 (2013) 481–490.
[38] J.N. Kim, I.Y. Chang, H.I. Kim, S.P. Yoon, Long-term effects of chitosan oligosaccharide in streptozotocin-induced diabetic rats, Islets 1 (2009) 111–116.
[39] C. Ju, W. Yue, Z. Yang, Q. Zhang, X. Yang, Z. Liu, et al., Antidiabetic effect and mechanism of chitooligosaccharides, Biol. Pharma. Bull. 33 (2010) 1511–1516.
[40] X. Dai, P. Chang, Q. Zhu, W. Liu, Y. Sun, S. Zhu, et al., Chitosan oligosaccharides protect rat primary hippocampal neurons from oligomeric beta-amyloid 1-42-induced neurotoxicity, Neurosci. Lett. 554 (2013) 64–69.